HHS Public Access
Author manuscript
Bioinform Biomed Eng (2019). Author manuscript; available in PMC 2020 March 09.

Published in final edited form as:
Bioinform Biomed Eng (2019). 2019 May ; 11466: 469–478. doi:10.1007/978-3-030-17935-9_42.

Cross Modality Microscopy Segmentation via Adversarial Adaptation

Yue Guo[1], **Qian Wang**[2], **Oleh Krupa**[3], **Jason Stein**[4], **Guorong Wu**[2], **Kira Bradford**[1], **Ashok Krishnamurthy**[1]

[1]Renaissance Computing Institute, Chapel Hill, NC, USA

[2]Department of Psychiatry, University of North Carolina at Chapel Hill, Chapel Hill, NC, USA

[3]Department of Biomedical Engineering, University of North Carolina at Chapel Hill, Chapel Hill, NC, USA

[4]Department of Genetics, University of North Carolina at Chapel Hill, Chapel Hill, NC, USA

Abstract

Deep learning techniques have been successfully applied to automatically segment and quantify cell-types in images acquired from both confocal and light sheet fluorescence microscopy. However, the training of deep learning networks requires a massive amount of manually-labeled training data, which is a very time-consuming operation. In this paper, we demonstrate an adversarial adaptation method to transfer deep network knowledge for microscopy segmentation from one imaging modality (e.g., confocal) to a new imaging modality (e.g., light sheet) for which no or very limited labeled training data is available. Promising segmentation results show that the proposed transfer learning approach is an effective way to rapidly develop segmentation solutions for new imaging methods.

Keywords

Transfer learning; Generative adversarial networks; Microscopy segmentation

1 Introduction

In the last decade, various cell segmentation methods have been developed for images from electron microscopy [18], confocal [9], and light sheet imaging [12]. Recently, there have also been successful applications of cell segmentation using deep learning techniques [16], such as U-Net [14].

It is well known that the success of deep learning is dependent upon having a substantial number of labeled training samples [3]. Manual labeling of training samples, however, is prohibitively expensive in terms of time and labor. Therefore, having a sufficient number of training samples presents a major challenge in developing an automatic cell segmentation algorithm for a new imaging modality.

yueguo@renci.org.

Various transfer learning methods [4, 6, 17] were proposed to tackle the lack of training data challenge. Notably, R-CNN [4] first proposed fine-tuning deep features to transfer deep representations from a labeled dataset to a dataset where the labels are limited. A similar approach was adopted for neonatal video analysis in [6]. Recent transfer learning methods rely on Generative Adversarial Network (GAN) [5], which consists of a discriminative model and a generative model, and they are trained in an adversarial fashion: the generative model generates data to confuse the discriminative model while the goal of the latter is to distinguish the generated data from the real data. This paradigm has been applied to the state-of-the-art transfer learning method by adversarial adaptation [17], i.e., minimizing the disparity between the two models so that they cannot differentiate between the source dataset (i.e., the existing labeled dataset) and target dataset (i.e., the unlabeled dataset). One drawback of this method is that the underlying deep neural network is LeNet which is designed for classification and is not suitable for image segmentation.

There have been several applications to leverage GAN-based approaches in the microscopy segmentation field [2, 15, 19]. In [15], a multi-scale GAN was proposed with post processing for bright-field microscopy image segmentation, while [2] developed a GAN architecture with multiple deep neural network blocks in the discriminator. However, both methods were trained in a supervised fashion and still required manually labeled data. [19] utilized GAN to model the gap between the labeled and unlabeled data, yet their iterative training process required the labeled and unlabeled data to come from the same modality, and this model cannot be extended to a cross-modality situation.

Our contribution is two-fold. First, we present an unsupervised solution for cross-modality microscopy segmentation, inspired by the adversarial adaptation method [17]. Specifically, we trained a segmentation model for light sheet images by utilizing confocal images. To further validate this model, we manually labeled a limited number of light sheet images for evaluation purposes. Secondly, we extended the adversarial adaptation method [17] by (a) replacing the underlying deep model with an optimized U-Net [14] to improve segmentation performance; and (b) incorporating batch normalization [8] to expedite the training process.

2 Related Work

Recent transfer learning work has witnessed much progress thanks to the success of deep learning [4–7, 17]. R-CNN [4] fine-tuned pre-trained deep features to transfer knowledge from an image classification dataset to an object detection dataset. [6] also utilized pre-trained deep features with a hidden Markov model for neonatal video analysis. [7] further extended the idea by averaging fine-tuned deep features from the K nearest categories to approximate the adaptations.

Generative Adversarial Network (GAN) [5] related work has been extensively explored for transfer learning. Prior work focused on generative tasks, e.g., DCGAN [13] used pre-trained discriminators in GAN to generate human face images or CGAN [11] introduced additional conditioning on both generators and discriminators in GAN to generate image tags. Later, CoGAN [10] applied GAN for transfer learning by proposing two independent GANs for source and target images to learn a joint distribution from different datasets. [17]

simplified CoGAN by removing the generative model of CoGAN and designed a discriminative model. However, these methods are tested on classification tasks and not suitable for microscopy segmentation.

Several methods have used GAN for microscopy segmentation [2, 15, 19]. [2] applied GAN by proposing a multiple input architecture in the discriminators of GAN, which takes as input both microscopy images and corresponding annotated segmentation. [15] extended GAN by replacing the generative model with a multi-scale segmentation network. One limitation of these method, however, is that they still require manually annotated images during training. [19] followed the dual-network structure in [15] and expanded it with an iterative training process, which could gradually update the segmentation network to generate correct results for images without manual annotations, but could not handle the cross-modality scenario.

Inspired by [17], our work applied GAN with an optimized U-Net [14] and batch normalization [8] for cross-modality microscopy segmentation.

3 Methods

Our work integrates an optimized U-Net [14] with adversarial adaptation [17]. In addition, batch normalization [8] is adopted to facilitate the training process. Each component of our proposed model is described in more detail in the following sections.

3.1 Adversarial Adaptation

Our unsupervised adversarial adaptation framework consists of three parts: a source model M_s, a target model M_t and an adversarial model M_a, as shown in Fig. 1. We assume that there is an existing source data set D_s with labels L_s that has been used to train a model M_s using supervised learning to an acceptable performance. In our case, D_s are confocal images and the labels L_s are binary assignments (nucleus/background) for each pixel in each of the images in D_s. The labels L_s are manually generated. Also given is the target dataset D_t, which is unlabeled. The goal of the adversarial adaptation framework is to create a model M_t that can assign labels (nucleus/background) to each pixel of each image in D_t. In our application, the images in D_t are light-sheet images. The adversarial network approach is thus used to transfer the knowledge from the model M_s to the model M_t. While we focus on transfer learning from confocal image segmentation to light sheet image segmentation in this case, this approach is generalizable to other cases. For example, D_s could be images with a particular setting of microscope acquisition parameters, while D_t could be the same imaging modality, but with a different setting of microscope acquisition parameters.

The source model is first trained using D_s and L_s. The loss function used in training is

$$\begin{aligned}\mathscr{L}_s(D_s, L_s, M_s) = & -\sum_{D_s} 1_{L = L_s} \log S(M_s(D_s)) \\ & -\sum_{D_s}\left(1 - 1_{L = L_s}\right)\log(1 - S(M_s(D_s))),\end{aligned} \tag{1}$$

which is a standard cross entropy function for a binary segmentation task. S represents the softmax layer, as illustrated in Fig. 1. The target and source model share the same architecture but are trained separately. The source model is trained using the labeled source data D_s, while the target model training is through adversarial adaptation.

The trained source model M_s is used to train the target model via adversarial adaptation. The objective of adversarial adaptation is to minimize differences of these two models so that the target model can learn a discriminative mapping from the source domain to the target domain. We use the GAN-based loss [5] for this goal

$$\mathscr{L}_a(D_s, D_t, M_t) = -\sum_{D_s} \log M_a(M_s(D_s)) - \sum_{D_t} \log(1 - M_a(M_t(D_t))) . \tag{2}$$

This is also a standard binary cross entropy loss function, where the label 1 and 0 are assigned for the source dataset and the target dataset, respectively.

In the training process, the parameters of the source model M_s is fixed to avoid oscillation [17] and M_s is also used for the initialization of the target model M_t. In addition, inverted labels [5], i.e., assigning opposite labels for source images and target images, were adopted using the loss function.

$$\mathscr{L}'_a(D_s, D_t, M_a) = -\sum_{D_t} \log M_a(M_t(D_t)) - \sum_{D_s} \log(1 - M_a(M_s(D_s))) . \tag{3}$$

In summary, we have two independent loss functions in the adversarial learning process. Equations 2 and 3 optimize the target model M_t , and the adversarial model M_a, respectively. The dual-loss-function setting proves to be an efficient training technique; using a single loss function can cause vanishing gradients [17].

3.2 U-Net

U-Net [14] consists of two networks, a contracting network and an upsampling network. This symmetric structure is capable of capturing precise localization information of the images, and can achieve state-of-the-art results on several datasets. One drawback of the network, however, is that it is unable to segment the boundary of images due to the pooling process. Therefore, we propose to use a sliding window approach to extensively scan the whole image and only segment the center pixel of the window. The filter size and layer number are adjusted based on the input image size. Figure 2 shows our optimized U-Net. We use this model as our implementation choice of M_s and M_t in Sect. 2. The TensorFlow model in [1] is used for implementation.

3.3 Batch Normalization

To mitigate the problem of covariate shift, our work also incorporates batch normalization [8], which uses the mean and variance within each batch to normalize the activation values of the non-linear layers so that the activation values can achieve a standard Gaussian distribution during training. A noticeable performance improvement was observed when applying this technique in the adversarial network M_a.

4 Dataset

We are continuing acquiring new data for research and we have obtained nine confocal images and four light sheet images so far. The confocal images (D_s) with a resolution of 800 × 600 (0.4613 × 0.4613 μm^2/pixel) were used to train the source model M_s. For each pixel in the confocal images, we extracted a 31 × 31 sub-image centered on that pixel, and then assigned the binary label of that pixel, i.e., nucleus or background, as the label for this sub-image. The same image batch generating paradigm was applied to the 620 × 520 (0.4853 × 0.4853 μm^2/pixel) light sheet images (D_t). To evaluate the effectiveness of the transfer learning, we used a limited set of manually-labeled data for the light sheet image. Example images are shown in Fig. 3. Please note that manually labeled light sheet images are *not* used in the training process.

5 Experiments

We conducted three sets of experiments to prove the effectiveness of our proposed model. We first performed an ablation study of our model with the state-of-the-art adversarial adaptation [17] as the baseline. Second, we compared our unsupervised method with the supervised state-of-the-art segmentation method, U-Net. Finally, we explored a bi-directional adaptation, i.e., from confocal images segmentation to light sheet image segmentation and vice versa. Sørensen-Dice similarity coefficient (DICE), $2TP/(2TP + FP + FN)$, was used to evaluate the segmentation performance. The adversarial model has 3 fully connected layers with Leaky ReLU activation function. All of the layers have 1024 hidden units with Batch Normalization. All of the models were trained over 10000 iterations with a batch size of 128 and no further improvement was observed.

5.1 Ablation Study

Adversarial adaptation [17] was employed as a baseline to validate the performance of the adversarial learning. [17] uses LeNet with ReLu activation function as the source and target model. We replaced the LeNet with our optimized U-Net and added batch normalization in the model. The results are provided in Table 1, which reveal the incremental improvement of our proposed approach.

5.2 Comparison with U-Net

For this experiment, we compared the performance of the proposed method with U-Net, which trained on light sheet images at a variety of settings in terms of the number of the available training samples. We had to reduce the size of the network by removing the last fully connected layer to avoid severe over-fitting. Table 2 presents the results of the supervised method. The results show that the performance of U-Net suffers when training data is limited while our proposed method can take advantage of data from other domains to tackle this problem.

5.3 Bi-Directional Adaptation

In addition to transfer the segmentation knowledge from confocal domain to light sheet domain, we conducted another experiment for the opposite domain, i.e. light sheet to confocal to further demonstrate the capabilities of our method. The results of this bi-directional experiment are shown in Table 3. Example visual results are also illustrated in Fig. 4.

6 Conclusion

This paper demonstrates the capabilities of an unsupervised adversarial adaptation framework for cross-modality transfer learning. Our model leverages the dataset from confocal images to train a segmentation model for light sheet images and achieves strong results in this challenging task. We also investigate the generality of our model by exploring bi-directional adaptation, indicating potential for other cross-modality applications in imaging research. Finally, our work shows promise in applying transfer learning to image segmentation problems in the neuroscience domain.

Acknowledgements.

This work was supported in part by the National Science Foundation under grants OCI-1153775 and OAC-1649916.

References

1. Akeret J, Chang C, Lucchi A, Refregier A: Radio frequency interference mitigation using deep convolutional neural networks. Astron. Comput 18, 35–39 (2017)
2. Arbelle A, Raviv TR: Microscopy cell segmentation via adversarial neural networks In: ISBI 2018, pp. 645–648. IEEE (2018)
3. Deng J, Dong W, Socher R, Li LJ, Li K, Fei-Fei L: ImageNet: a large-scale hierarchical image database In: CVPR, pp. 248–255. IEEE (2009)
4. Girshick R, Donahue J, Darrell T, Malik J: Rich feature hierarchies for accurate object detection and semantic segmentation. In: CVPR, pp. 580–587 (2014)
5. Goodfellow I, et al.: Generative adversarial nets. In: NIPS, pp. 2672–2680 (2014)
6. Guo Y, Wrammert J, Singh K, Ashish K, Bradford K, Krishnamurthy A: Automatic analysis of neonatal video data to evaluate resuscitation performance In: ICCABS, pp. 1–6. IEEE (2016)
7. Hoffman J, et al.: LSDA: large scale detection through adaptation. In: Advances in Neural Information Processing Systems, pp. 3536–3544 (2014)
8. Ioffe S, Szegedy C: Batch normalization: accelerating deep network training by reducing internal covariate shift. In: ICML, vol. 37, pp. 448–456. PMLR (2015). http://proceedings.mlr.press/v37/ioffe15.html
9. Liu M, et al.: Adaptive cell segmentation and tracking for volumetric confocal microscopy images of a developing plant meristem. Mol. Plant 4(5), 922–931 (2011) [PubMed: 21965456]
10. Liu MY, Tuzel O: Coupled generative adversarial networks. In: NIPS, pp. 469–477 (2016)
11. Mirza M, Osindero S: Conditional generative adversarial nets. arXiv preprint arXiv:1411.1784 (2014)
12. Packard RRS, et al.: Automated segmentation of light-sheet fluorescent imaging to characterize experimental doxorubicin-induced cardiac injury and repair. Sci. Rep 7(1), 8603 (2017) [PubMed: 28819303]
13. Radford A, Metz L, Chintala S: Unsupervised representation learning with deep convolutional generative adversarial networks. arXiv preprint arXiv:1511.06434 (2015)

14. Ronneberger O, Fischer P, Brox T: U-Net: convolutional networks for biomedical image segmentation In: Navab N, Hornegger J, Wells WM, Frangi AF (eds.) MICCAI 2015. LNCS, vol. 9351, pp. 234–241. Springer, Cham (2015). 10.1007/978-3-319-24574-4_28

15. Sadanandan SK, Karlsson J, Wählby C: Spheroid segmentation using multi-scale deep adversarial networks In: ICCVW, pp. 36–41. IEEE (2017)

16. Shen D, Wu G, Suk HI: Deep learning in medical image analysis. Ann. Rev. Biomed. Eng 19(1), 221–248 (2017). pMID: 28301734 [PubMed: 28301734]

17. Tzeng E, Hoffman J, Saenko K, Darrell T: Adversarial discriminative domain adaptation. In: CVPR, vol. 1, p. 4 (2017)

18. Yang HF, Choe Y: Cell tracking and segmentation in electron microscopy images using graph cuts In: ISBI, pp. 306–309. IEEE (2009)

19. Zhang Y, Yang L, Chen J, Fredericksen M, Hughes DP, Chen DZ: Deep adversarial networks for biomedical image segmentation utilizing unannotated images. In: Descoteaux M, Maier-Hein L, Franz A, Jannin P, Collins DL, Duchesne S (eds.) MICCAI 2017. LNCS, vol. 10435, pp. 408–416. Springer, Cham (2017). 10.1007/978-3-319-66179-7_47

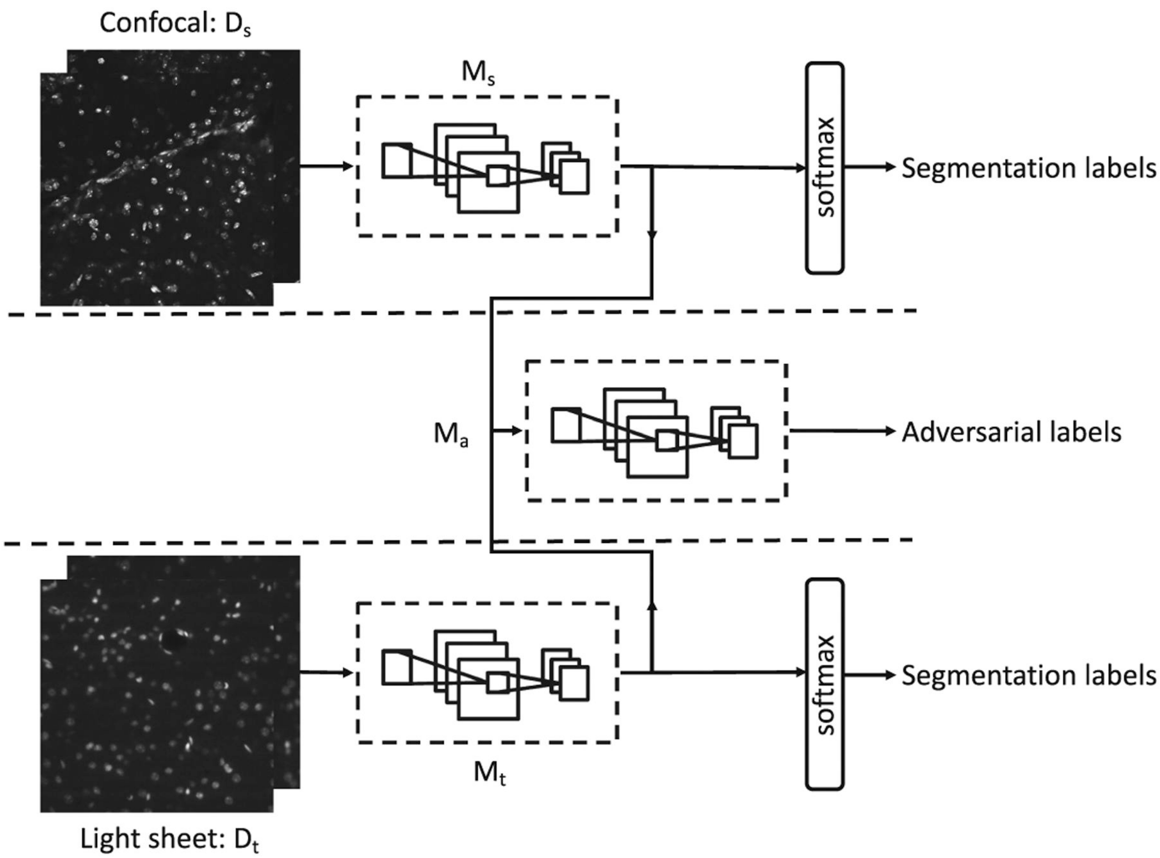

Fig.1.

The overview of the proposed framework. Note that M_s and M_t share the same deep network structure (number of layers, number of units, connectivity), while M_a can have a different structure

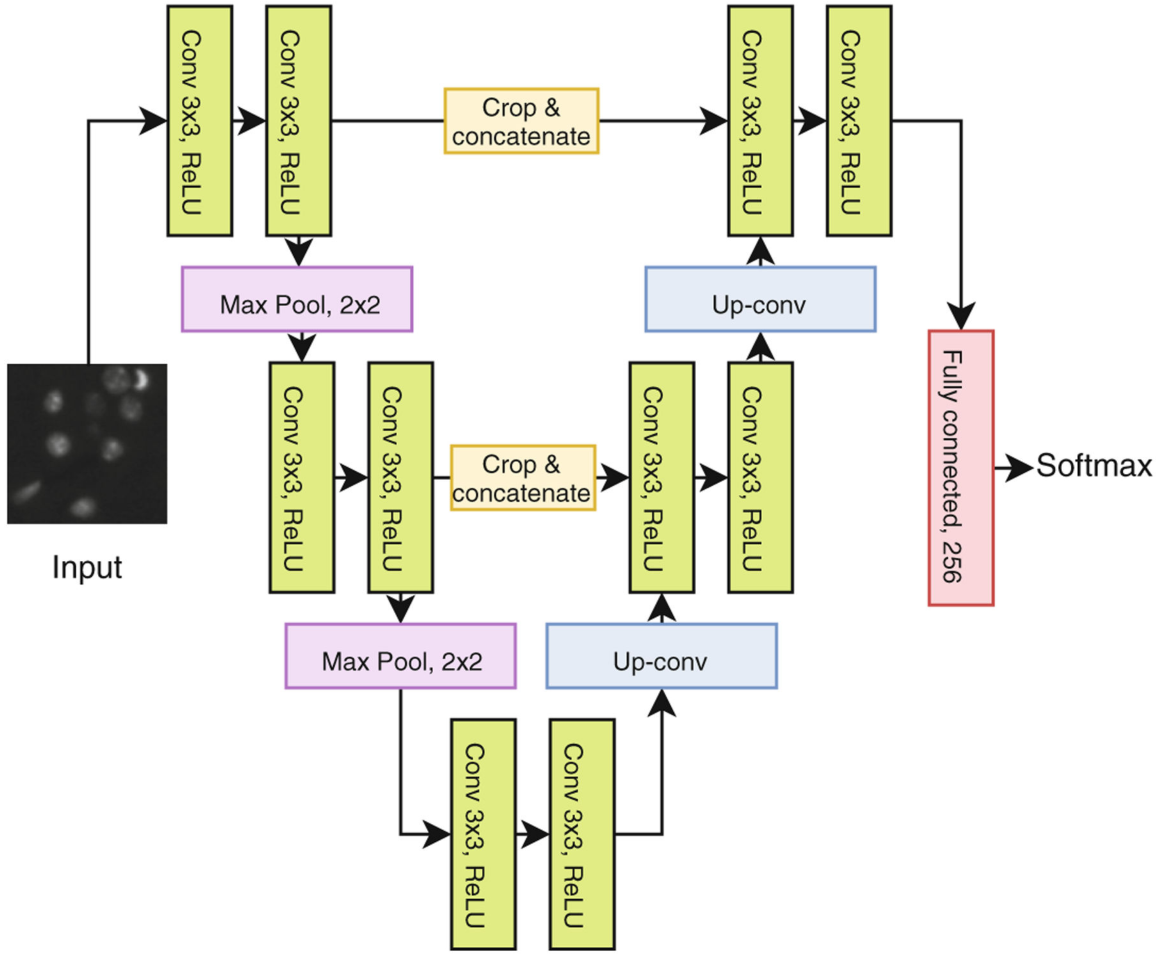

Fig.2.
The structure of our optimized U-Net

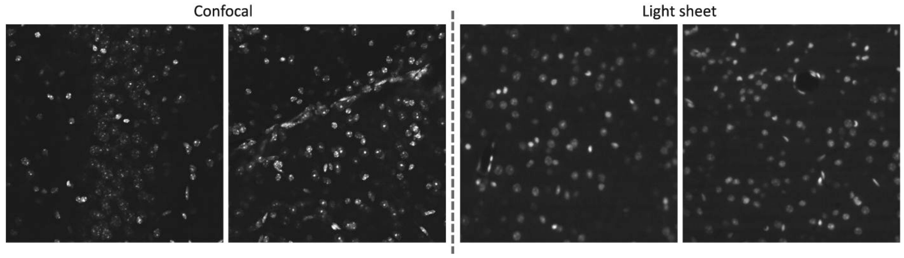

Fig.3.
Example confocal (left) and light sheet (right) images

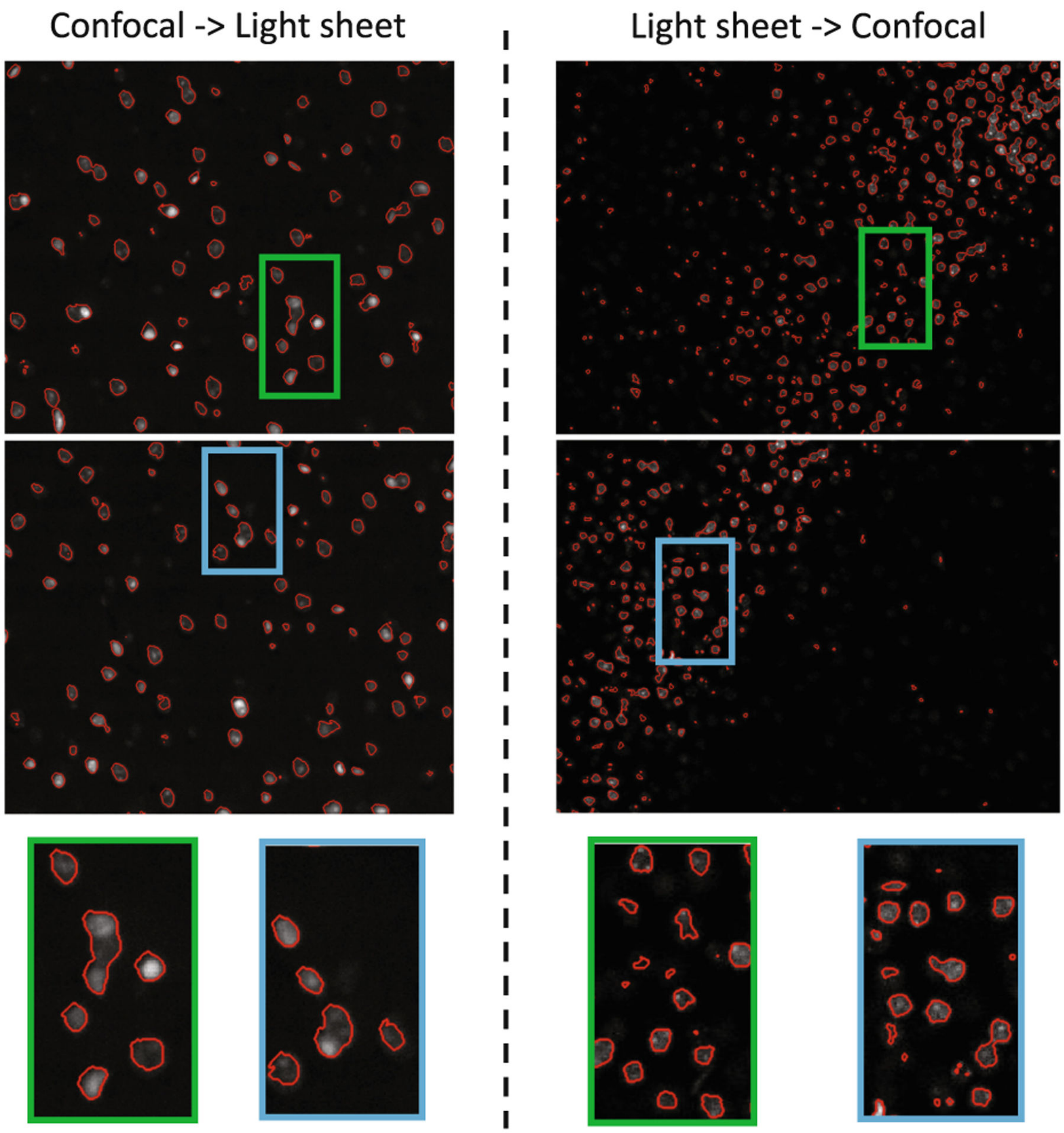

Fig.4.

Segmentation results of our adversarial adaption model: confocal domain to light sheet domain (left) and light sheet domain to confocal domain (right). The red contour obtained using MATLAB imcontour function on the binary segmentation predictions. The bottom row shows the zoomed results.

Table 1.

Experimental results of unsupervised adaption from confocal images to light sheet images. Light sheet image labels were NOT used in either experiment

Experimental settings	**DICE**
Adversarial adaptation [17]	0.593
Adversarial adaptation + U-Net	0.672
Adversarial adaptation + U-Net + Batch Normalization	0.709

Author Manuscript

Author Manuscript

Author Manuscript

Table 2.

Experimental results of supervised methods and our unsupervised method. For the supervised methods, cross validation is applied and averaged results are shown

Model	Experimental settings	DICE
U-Net	Trained on 1 light sheet images, tested on 3 light sheet images	0.577
U-Net	Trained on 3 light sheet images, tested on 1 light sheet image	0.676
Ours	Tested on 4 light sheet images	0.709

Table 3.

Experimental results of Bi-directional adaptation

Source domain	Target domain	DICE
Confocal	Light sheet	0.709
Light sheet	Confocal	0.680